Engineering of Targeted Nanoparticles for Cancer Therapy Using Internalizing Aptamers Isolated by Cell-Uptake Selection

Zeyu Xiao,[†,‡,¶] Etgar Levy-Nissenbaum,[†,‡,¶] Frank Alexis,[†,‡] Andrej Lupták,[⊥] Benjamin A. Teply,[†,‡] Juliana M. Chan,[§,∥] Jinjun Shi,[†,‡] Elise Digga,[†] Judy Cheng,[†,‡] Robert Langer,[‡,§] and Omid C. Farokhzad*[,†,‡]

[†]Laboratory of Nanomedicine and Biomaterials, Department of Anesthesiology, Brigham and Women's Hospital, Harvard Medical School, Boston, Massachusetts 02115, United States, [‡]MIT-Harvard Center for Cancer Nanotechnology Excellence and [§]The David H. Koch Institute for Integrative Cancer Research, Massachusetts Institute of Technology, Cambridge, Massachusetts 02139, United States, [⊥]Department of Molecular Biology and Center for Computational and Integrative Biology, Massachusetts General Hospital, Harvard Medical School, Boston, Massachusetts 02114, United States, and [∥]Department of Biology, Massachusetts Institute of Technology, Cambridge, Massachusetts 02139, United States. [¶]These authors contributed equally to this work.

ABSTRACT

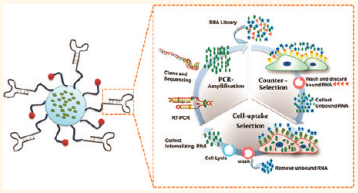

One of the major challenges in the development of targeted nanoparticles (NPs) for cancer therapy is to discover targeting ligands that allow for differential binding and uptake by the target cancer cells. Using prostate cancer (PCa) as a model disease, we developed a cell-uptake selection strategy to isolate PCa-specific internalizing 2′-O-methyl RNA aptamers (Apts) for NP incorporation. Twelve cycles of selection and counter-selection were done to obtain a panel of internalizing Apts, which can distinguish PCa cells from nonprostate and normal prostate cells. After Apt characterization, size minimization, and conjugation of the Apts with fluorescently labeled polymeric NPs, the NP—Apt conjugates exhibit PCa specificity and enhancement in cellular uptake when compared to nontargeted NPs lacking the internalizing Apts. Furthermore, when docetaxel, a chemotherapeutic agent used for the treatment of PCa, was encapsulated within the NP—Apt, a significant improvement in cytotoxicity was achieved in targeted PCa cells. Rather than isolating high-affinity Apts as reported in previous selection processes, our selection strategy was designed to enrich cancer cell-specific internalizing Apts. A similar cell-uptake selection strategy may be used to develop specific internalizing ligands for a myriad of other diseases and can potentially facilitate delivering various molecules, including drugs and siRNAs, into target cells.

KEYWORDS: nanoparticles · internalization · *in vitro* selection · aptamer · targeted cancer therapy

Targeted nanoparticle (NP) therapeutics have shown great potential for cancer therapy, as they provide enhanced efficacy and reduced side effects.[1−3] These features are mainly due to the improved accumulation of NPs in tumors and active intracellular delivery of NPs into cancer cells. Indeed, intracellular delivery of NP therapeutics results in higher drug concentration inside the cells and, thus, is more efficacious than noninternalized nanotherapeutics.[4−6] In addition, intracellular NP delivery is particularly important for the development of nucleic acid-based therapeutics (*e.g.*, genes and siRNAs), as these macromolecules cannot readily cross the cell membrane.[7]

For intracellular delivery of NPs, one strategy is to modify their physicochemical properties, such as surface topography and charge, allowing for rapid NP internalization.[8] This strategy has the limitation of nonspecificity whereby NP uptake occurs indiscriminately. The other strategy is to incorporate NPs with targeting ligands, which enhance cellular uptake *via* receptor-mediated endocytosis and provide cell-targeting specificity.[1] Most targeted NPs under preclinical and clinical development utilize ligands that are isolated from well-characterized cancer antigens. However, only limited number of antigens have been characterized for cancer cell recognition,[9] and some of these characterized antigens cannot mediate the internalization of their assoaciated ligands. Therefore, a robust targeted internalizing NP delivery platform needs to be established where development can be achieved without precharacterization of target antigens.

Recently, aptamers (Apts) have emerged as a promising class of ligands for targeted NP delivery.[3,10,11] Apts are single-stranded RNA or DNA oligonucleotides that fold into three-dimensional conformations with high binding affinity and specificity. They have shown low immunogenicity. The relatively small size of Apts allows for more efficient penetration into biological compartments.[12] Moreover, Apts can be manipulated and

* Address correspondence to ofarokhzad@zeus.bwh.harvard.edu.

Received for review October 28, 2011 and accepted December 14, 2011.

Published online January 03, 2012
10.1021/nn204165v

produced by a chemical synthesis process, which is less prone to batch-to-batch variability than other biologic products.[13] Because of these favorable features, we used Apts as model ligands to develop a targeted internalizing NP–Apt platform.

To achieve this goal, we designed a unique selection strategy to enrich internalizing Apts for NP incorporation. First, we chose to isolate Apts directly against live cancer cells, and thus the evolved Apts can recognize cancer cells without precharacterization of the targeted cancer antigens. Using this strategy, a single selection process potentially generates Apts that can target multiple antigens on cancer cells, which in turn yields a diverse candidate pool of Apts facilitating multiantigen targeting. Second, stringent counter-selections were used to remove Apt candidates that interacted with nontarget cells, contributing to the target-cell specificity of the evolved Apts. Most importantly, the selection was specially designed to enrich internalizing Apts rather than highest affinity Apts as reported in previous SELEX (systematic evolution of ligands by exponential enrichment) processes,[14–18] which may evolve Apts that have bound to cells without internalizing. For example, Shangguan *et al.* systematically developed "cell-SELEX" strategy wherein the selection was performed at 4 °C to enrich Apts that specifically bound to target cells.[17,19] Among the more than 30 isolated Apts, only one Apt was reported to have the internalization feature.[20] Some other isolated Apts bind to target cells at 4 °C, whereas they lose their binding capabilities at 37 °C, which could hinder their applications as drug delivery vehicles.[21] Toward the specific goal, we performed the selection at physiological temperature (37 °C), where cells and their membrane receptors are biologically active and continue to function in endocytosis. Additionally, we selectively collected internalizing Apts after removing noninternalized membrane-bound Apts. Moreover, the isolated RNA Apts were introduced with 2′-O-methyl (OMe) modification during the selection process, which facilitates the resistance of nuclease degradation inside the intracellular environments.[22] Characterized by the cellular uptake of the Apts, we termed the process "cell-uptake selection" (Figure 1).

As the proof-of-concept demonstration of cell-uptake selection, we isolated herein cell-specific internalizing 2′-OMe RNA Apts against prostate cancer (PCa) cells. The selected PCa-specific internalizing Apts were further characterized and conjugated to drug-encapsulated NPs for targeted PCa therapy.

RESULTS AND DISCUSSION

To demonstrate the robust and predictable features of our selection strategy, we performed two distinct but identical selections against PC3 and LNCaP cells. They represent two distinct PCa epithelial cell lines that differ

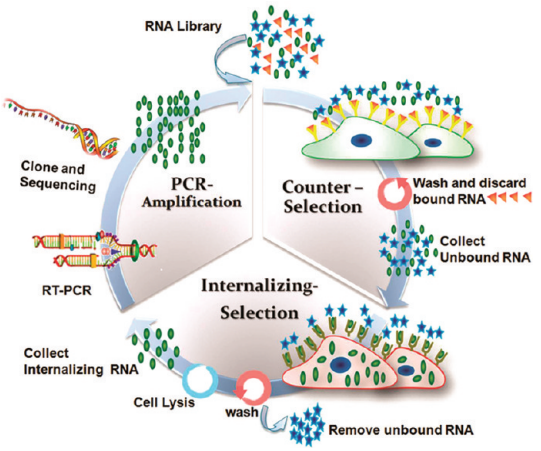

Figure 1. Schematic protocol of cell-uptake selection for evolving PCa-specific internalizing Apts. The 2′-OMe-RNA pools, transcribed from an initial DNA library, were incubated with prostate normal cells (counter-selection). After washing, the unbound RNAs were presented to PCa cells for binding and cell uptake. After washing or trypsin treatment and cell lysis, those internalizing RNAs were extracted (cell-uptake selection). The collected RNAs, after reverse transcription, were amplified by PCR. The PCR products were transcribed into 2′-OMe-modified RNAs for the next round of selection or cloned and sequenced for Apt identification in the last round selection.

in their androgen responsiveness: androgen-dependent (LNCaP) and androgen-independent (PC3). RWPE-1 (prostate normal epithelial cell line), BPH-1 (prostate benign hyperplastic epithelial cell line), and PrEC (prostate normal epithelial cell line) have differential surface antigen expression as compared with LNCaP or PC3[23] and serve as model counter-selection cell lines to prevent the collection of RNAs that could bind to common surface antigens present on noncancer cells. The starting RNA Apt candidate library was composed of 77 base long degradation-resistant RNA oligonucleotides incorporating GTP, 2′-OMe-ATP, 2′-OMe-CTP, and 2′-OMe-UTP.[24] The partly 2′-OMe-modified oligonucleotides were initially incubated with counter-selection cell lines (RWPE-1, BPH-1, and PrEC) consecutively, and the RNA sequences remaining in the supernatant were continually collected. The collected RNAs were incubated with the target cells (either PC3 or LNCaP) at 37 °C to allow for binding and cellular uptake. The cells were then extensively washed (rounds 1–12) and either lysed to collect the internalized RNAs (rounds 1–6) or treated with trypsin to remove the majority of membrane-bound RNAs prior to cell lysis and collection of internalized RNAs (rounds 7–12). The stringency of the selection was slowly increased by diminishing both the number of PC3 and LNCaP cells and the incubation time during the selection (rounds 1–12) and further increased by complicating the RNA pools through mutagenic PCR (round 7).[25] The progress of selection, measured by the number of PCR cycles needed to amplify the chosen material for the next round, is shown in Figure S1

(Supporting Information). As rounds of selection progressed, the needed PCR cycle number steadily decreased from the third round but did not decrease from 10th up to 12th round, thus indicating the saturation of Apt candidate enrichment.

Prior to identification of specific sequences in the round 12 RNA pool, we first confirmed that the enriched RNA pools (round 12 LNCaP and round 12 PC3), which represent many distinct Apt candidates, could be internalized and transported with NPs into target cancer cells. As a model NP platform, we used the hybrid lipid−polymer NP that has been designed and systematically investigated by our group.[26−28] The hybrid NP consists of (i) a poly(D,L-lactide-*co*-glycolide) (PLGA) hydrophobic core for drug encapsulation, (ii) a lipid monolayer, and (iii) a poly(ethylene glycol) (PEG) shell. PEG was conjugated to 1,2-distearoyl-*sn*-glycero-3-phosphoethanolamine (DSPE) at one end for interspersing into the lipid monolayer and was functionalized with a maleimide group at the other end for targeting ligand modification. This hybrid NP is prepared in a single-step process *via* nanoprecipitation and self-assembly, and the yielded NP has the size of 50−100 nm and ζ-potential of −10 to −20 mV, providing favorable physicochemical properties for drug delivery application. The conjugation of NP to the RNA pool relies on maleimide-thiol chemistry (Figure 2A). Briefly, the vicinal hydroxyl groups in the unmodified 5′-end GTP of the RNA pool were oxidized into aldehyde groups by periodate. These aldehyde groups further reacted with a free amine group of cystamine to introduce thiol groups. The resulting thiolated RNA pools were then incubated with maleimide-functionalized NPs encapsulating NBD (22-(*N*-(7-nitrobenz-2-oxa-1, 3-diazol-4-yl)amino)-23,24-bisnor-5-cholen-3β-ol) to form NP (NBD)−RNA pool conjugates. As demonstrated in Figure 2B, the presence of the selected LNCaP or PC3 round 12 pool greatly facilitated the uptake of the green fluorescent NPs into the target LNCaP or PC3 cells, separately. By contrast, control NPs similarly conjugated with the initial random library were not taken up by target cells at detectable levels. Figure 2C represents a panel of images across the *Z*-axis of a single cell with 3-D image deconvolution, demonstrating the intracellular source of fluorescent signal, consistent with NP uptake within LNCaP or PC3 cells. The cell-uptake selection was shown to have successfully enriched a pool of Apt candidates that are specifically internalized by PCa cells.

We next separately cloned and sequenced the enriched PC3 and LNCaP round 12 pools by using high-throughput genome sequencing methods. The sequences were sorted into putative families by aligning consensus motifs and termed XEO1, XEO2, ..., *etc.* XEO2, XEO9, and their homologues represented 12% and 10% of the selected 68 sequences in the PC3 round 12 pool, separately. XEO6 and its homologues

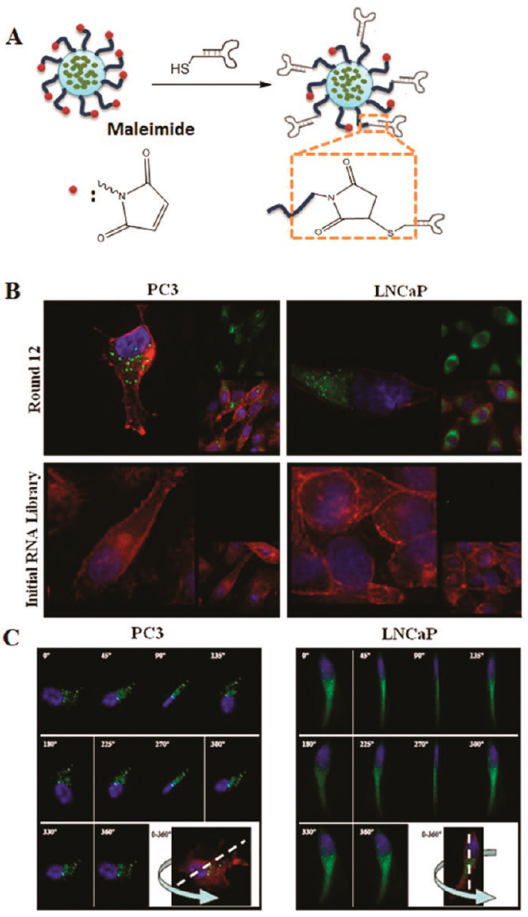

Figure 2. Demonstration of the internalization of NPs conjugated with round 12 RNAs. (A) RNAs and NPs were conjugated by using maleimide-thiol chemistry. (B) Cellular uptake of NP−round 12 RNA conjugates. In all of the images, the nucleus is in blue (DAPI), cytoskeleton is in red (rhodamine phalloidin), and NP is in green (NBD dye). Top left: NP-PC3 round12 RNA conjugates in PC3 cells. Bottom left: NP−initial RNA library conjugates in PC3 cells. Top right: NP-LNCaP round 12 RNA conjugates in LNCaP cells. Bottom right: NP−initial RNA library conjugates in LNCaP cells. (C) Three-dimensional reconstruction of cell images confirm that the NP−round 12 RNA conjugates are inside the PC3 cells (left) and LNCaP cells (right).

represented 14% of the selected 65 sequences in the LNCaP round 12 pool. These three abundant sequences, along with their truncated forms (XEO2 mini and XEO6 mini, described in Supporting Information, Figure S2), were considered as the best internalizing Apt candidates for further characterization (Table 1).

We proceeded to characterize the internalization of the selected Apts. Because specific sequences had been identified, the synthesis, modification, and labeling of Apts were directly performed by RNA synthesizers. This solid-phase chemical synthesis process is straightforward and accessible to be scaled up. Cy3-labeled Apts were incubated with target cells (PC3 or LNCaP) at 37 °C for 2 h to allow for cellular uptake. Cells were then treated with trypsin to remove the external binding fluorescence signal that could interfere with the detection of the intracellular Apts,[20,29] followed by

TABLE 1. Sequences of selected internalizing Apts

aptamer source			
PC3 round 12	LNCaP round 12	size	sequences
XEO2		77	5′-GG GAG AGG AGA GAA ACG UUC UCG CUG ACU GAC CUG GCG AGG AUU GAC GCU GAU GGA UCG UUA CGA CUA GCA UCG AUG-3′
XEO2 mini		34	5′-CAC GAC GCU GAU GGA UCG UUA CGA CUA GCA UCG C-3′
	XEO6	77	5′-GG GAG AGG AGA GAA ACG UUC UCG GGC GCG AGA CGA UCC GCU AUG AUG GCU GUG GGA UCG UUA CGA CUA GCA UCG AUG-3′
	XEO6 mini	50	5′-CGG GCG CGA GAC GAU CCG CUA UGA UGG CUG UGG GAU CGU UAC GAC UAG CA-3′
XEO9		77	5′-GG GAG AGG AGA GAA ACG UUC UCG UUU GUG AAU ACG CGC GUU GUC CCU UGA GUG GGA UCG UUA CGA CUA GCA UCG AUG-3′

flow cytometry analysis. Cells were incubated with similarly synthesized Cy3-labeled initial RNA random library as a control and trypsinized to determine nonspecific background uptake. Figure 3 shows the representative results from one of the selected Apts (XEO2). Compared with the initial library, the XEO2 profile showed a clear right shift in cytometric analysis, suggesting uptake by PC3 cells (Figure 3A). We further evaluated uptake of Cy3-labeled XEO2 during 2 h incubation with various concentrations. The internalization of XEO2 was enhanced in a concentration-dependent fashion and reached a plateau in target PC3 cells (Figure 3B). By comparison, uptake of the initial library showed only a slight linear increase. The difference in the cellular uptake profiles indicates that, unlike the nonspecific cellular uptake shown by random sequences, receptor-mediated endocytosis might participate in the specific and efficient cellular uptake of XEO2.[29−31] Confocal images further confirmed the cellular internalization of Cy3-labeled XEO2 (Figure 3C).

Besides XEO2, the other selected sequences also exhibited cellular uptake into target cancer cells (Table 2; additional examples are shown in Figures S3, S4, and S6 in Supporting Information). Using *R* value as the criteria (Table 2) to measure internalization capacity, we quantitatively compared selected Apts with a well-studied A10 Apt that binds to prostate-specific membrane antigen (PSMA). A10 gets taken up into PSMA-expressed cells such as LNCaP but not PC3 cells that do not express PSMA antigens. As shown in Figure S7 (Supporting Information), the *R* value of A10 in LNCaP cells was 1.45 ($1 < R < 1.5$, ++). As such, the internalization capacity of XEO2, XEO6, XEO6 mini (XEO6 truncated form), and XEO9 ($R > 2$, ++++, as summarized in Table 2) was higher than that of A10 ($1 < R < 1.5$, ++) in LNCaP cells, indicating the robust feature of "cell-uptake selection" strategy. In addition, our strategy allows, for the first time, to discover a group of new internalizing Apts XEO2, XEO2 mini, and XEO9, which can get taken up into PC3 cells with high internalization capacity ($R > 2$, ++++, as summarized in Table 2). To the best of our knowledge, no cancer antigens and targeting Apt ligands have currently been identified for PC3 cells.[32] Our strategy has the advantage for enabling the design and engineering of ligand-targeted NPs without prior knowledge of target antigens.

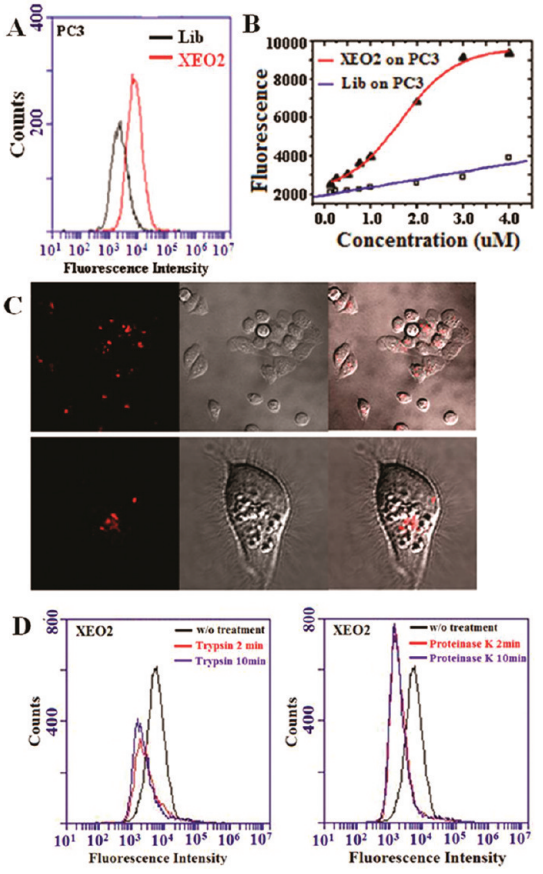

Figure 3. Internalization of Apt XEO2. (A) Representative flow cytometric profiles showing XEO2 internalization signals in PC3 cells. The black curve represents the background uptake of unselected initial library. (B) Uptake efficiency of XEO2 by PC3. Cy3-labeled XEO2 was incubated with target cells at different concentrations. Fluorescence signals from inside cells were determined by flow cytometry. (C) Representative confocal images showing the distributions of Cy3-labeled XEO2 inside PC3 cells. Left: fluorescence image. Middle: wide-field image. Right: overlay of fluorescence and wide-field images. (D) Effects of trypsin (left) and proteinase K (right) treatment on the binding of XEO2. The PC3 cells were pretreated with trypsin or proteinase K for 2 or 10 min before incubation with XEO2.

To ascertain whether these Apts were binding to cell-surface membrane proteins, cells were pretreated with proteases, including trypsin and proteinase K, before incubation with Cy3-labeled Apts. For example, although XEO2 showed the binding affinity of 117 nM with PC3 cells (Figure S5 of the Supporting Information), it lost the

TABLE 2. Cellular Uptake of Selected Apts by Different Cell Lines[a]

cell lines	cell source	XE02	XE02 mini	XE06	XE06 mini	XE09
PC3	prostate carcinoma (androgen-independent)	++++	++++	+	+	++++
LNCaP	prostate carcinoma (androgen-dependent)	++++	+	++++	++++	++++
RWPE-1	prostate normal epithelial	++	----	----	----	++
BPH	prostate benign hyperplastic epithelial	++	+	----	----	++
HeLa	cervical carcinoma	----	----	----	----	----
SKBR3	breast carcinoma	+	+	+	+	+
A375	melanoma	----	----	----	----	----
U373MG	brain glioblastoma-astrocytoma	----	----	----	----	----
T98G	brain glioblastoma	----	----	----	----	----
U87MG	brain glioblastoma-astrocytoma	----	----	----	----	----
A549	lung carcinoma	----	----	----	----	----
SKOV3	ovary adenocarcinoma	----	----	----	----	----

[a] Note: the internalization capacity of selected Apts in different cell lines was evaluated by *R* value as the following threshold. The mean fluorescence of selected sequence (MF sequence) in the FACS analysis was normalized to the mean fluorescence of initial library (MF lib) in the same experimental condition. $R = (\text{MF sequence} - \text{MF lib})/\text{MF lib}$. ----, $R < 0.5$; +, $0.5 \leq R \leq 1$; ++, $1 < R < 1.5$; +++, $1.5 \leq R < 2$; ++++, $R > 2$.

binding characteristics against target cells after protease treatments (Figure 3D), indicating that its target molecules are most likely membrane proteins. Protease treatment assays similarly showed the other selected Apts likely bound to membrane proteins (Figure S8 of the Supporting Information). Further characterization of the protein could lead to the discovery of novel PCa biomarkers.

Taken together, multiple internalizing Apts targeting the same cancer cells were generated from a single selection process. Using multiple Apts for development of NP–Apt conjugates may be most clinically useful, whereas conventional single antigen-targeted NP platforms may be confounded by the heterogeneous pattern of intra- and intertumoral antigen expression.[33,34] Such a group of internalizing Apts isolated from our designed selection can collectively interact with multiple antigens on cancer cells and potentially be utilized to develop a multiantigen targeted NP platform to address this limitation.

We subsequently assessed the cell-type specificity of selected internalizing Apts. As illustrated in Table 2, Apts XEO2 and XEO9 showed specific uptake into both LNCaP and PC3 cells. Apts XEO6 and XEO6 mini showed specific uptake only into LNCaP cells. Apt XEO2 mini showed specific uptake only into PC3 cells. All of these five sequences showed much less favorable uptake into other cell lines, including BPH, RWPE-1, HeLa, SKBR3, A375, U373MG, T98G, U-87MG, A549, and SKOV-3. The slight uptake into some of these cell lines may be due to the fact that some biomarkers, which are expressed in PCa cells, are also expressed in nonprostate cancer cells, albeit at a relatively lower expression level. For example, PSMA overexpressed in PCa cells is also expressed at various degrees in normal prostate and other normal tissues, including whole brain, kidney, liver, and small intestine,[35] and is similarly overexpressed on the neovasculature of most nonprostate solid tumors.[36,37] The XEO2 mini, XEO6, and XEO6 mini had the most specific internalization profiles among the selected Apts and thus may be promising for targeted delivery applications.

To investigate the feasibility of using the selected internalizing Apts for NP incorporation into potential applications, we used the XEO2 mini as a representative Apt to develop a model system of NP–Apt conjugates. The conjugation of Apt XEO2 mini and NP was achieved by using maleimide-thiol chemistry: the Apt was modified by solid-phase synthesis with a thiol group at its 5′-end, and the NP was prefunctionalized with maleimide. We previously have demonstrated the optimal density of A10 Apt on the NP surface for *in vitro* and *in vivo* efficacy.[38] With the determined optimal density of one Apt per 1180 nm^2 of NP surface area,[38] we anticipate our NPs with a diameter of 80 nm have approximately the density of 17 Apts per NP. We visualized the cellular uptake of the NP–Apt XEO2 mini (NP–Apt) by encapsulating NBD inside the NPs; though for clinical applications, small molecule drugs, siRNAs, or other therapeutics may be encapsulated. PC3 and HeLa cells were employed as model target and nontarget cell lines, respectively. As shown in Figure 4A, the cellular uptake of NP(NBD)–Apt was significantly enhanced in the target cells compared with that of the nonconjugated NP(NBD). The differential uptake of the NP(NBD)–Apt was not observed in the nontarget cells. The background NBD signal represented nonspecific cellular uptake of NPs and any free NBD released from the NPs during incubation. The high-magnification imaging (Figure 4B) shows the cellular uptake and cytoplasmic distribution of the NP(NBD)–Apt inside the target cells. In addition, flow cytometry analysis was performed to confirm specific cellular uptake of the targeted NP–Apt (Figure S9 of the Supporting Information).

With the model system of the XEO2 mini-conjugated NPs, we next investigated its potential efficacy for drug delivery by encapsulating docetaxel (Dtxl) inside the NPs. A control experiment was first performed by

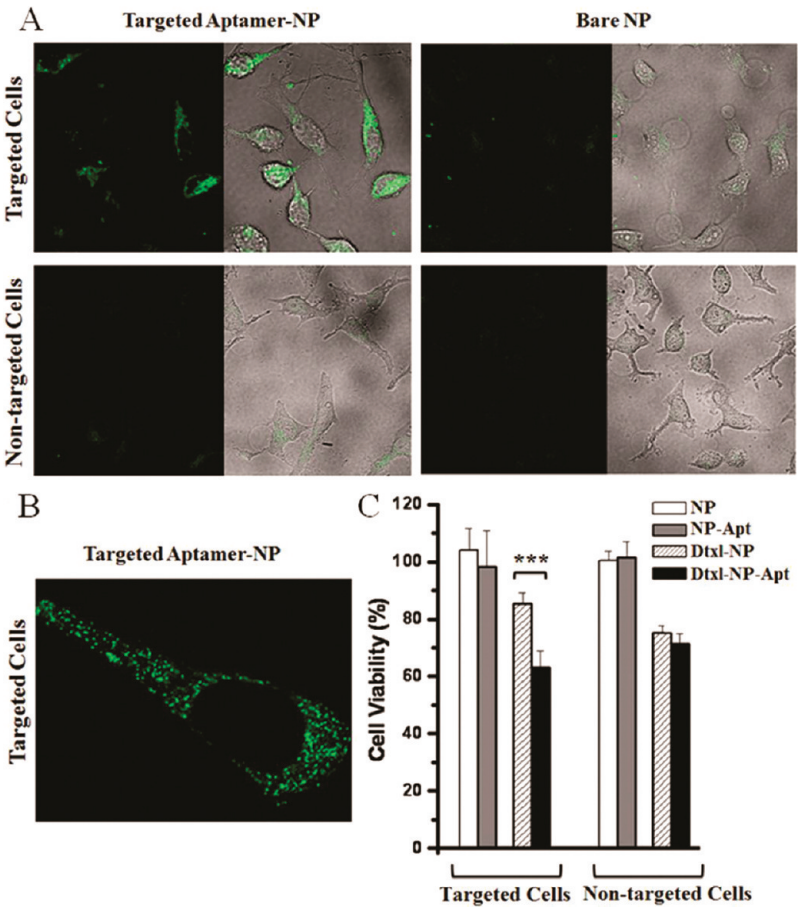

Figure 4. (A) Representative confocal images showing specific uptake of NP−XEO2 mini conjugates in different cells. NBD cholesterol is encapsulated in the NP. In each image, left panel is the fluorescent image, and right panel is the overlay of fluorescence and optical image. Targeted NP−XEO2 mini (left) and bare NP (right) were incubated with target PC3 cells (top) and nontarget HeLa cells (bottom). (B) Cellular distributions of NP−XEO2 mini (NBD) in PC3 cells by high-magnification confocal imaging. (C) Cytotoxicity study of Dtxl-encapsulated NP−Apt conjugates (Dtxl−NP−Apt), Dtxl-encapsulated NP without Apt (Dtxl−NP), NP−Apt conjugates without Dtxl (NP−Apt), and control NP without Dtxl (NP). ***, $P < 0.001$ by two sample student's *t* test.

incubating the cells with Apt XEO2 mini or NPs without drug in both nonconjugated and Apt-conjugated forms. No obvious cytotoxicity was found in either target or nontarget cell lines (Figure 4C and Figure S10 of the Supporting Information), confirming the noncytotoxicity of NPs and Apt XEO2 mini. After loading with Dtxl, we observed the differential cytotoxicity of Dtxl−NP in nontarget and target cells, which may be due to the differences in the nonspecific uptake of NPs and in the IC_{50} of Dtxl between two cell lines.[39−41] To exclude these intrinsic factors, we compared the cytotoxic effects of Dtxl−NP−Apt and Dtxl−NP in the same cell line, and thus each line is its own control. As shown in Figure 4C, the Dtxl−NP−Apt (71.45 ± 3.60%) showed similar cytotoxicity to the Dtxl−NP (75.33 ± 2.21%) in nontarget cells (mean ± SD, $n = 5$, $P > 0.05$). In contrast, the Dtxl−NP−Apt (63.10 ± 5.81%) was significantly more cytotoxic than the Dtxl−NP (85.47 ± 3.65%) in target cells (mean ± SD, $n = 5$, $P < 0.001$). The significant increase in cellular cytotoxicity is presumably through Apt-targeted intracellular delivery and release of Dtxl in target cells. Previously, we had developed Dtxl-encapsulated and A10 Apt-targeted NP that bound to the extracellular domain of the PSMA protein on the surface of PCa cells and explored the efficacy of this system *in vitro* and *in vivo*.[3] In that study, we showed an enhancement in the cytotoxicity of A10-conjugated Dtxl−NP−Apt (42 ± 2%) compared with Dtxl−NP lacking the A10 Apt (61 ± 5%).[3] Our newly developed internalizing NP−Apt system showed at least equivalent or more favorable enhancement in therapeutic efficacy than A10 Apt-targeted NP delivery system, demonstrating the potential of this system for targeted cancer therapy. More importantly, unlike the A10-targeted NPs which recognized the well-characterized PSMA protein, the current platform allows us to develop equally efficacious or better targeted NPs even when the target antigen is unknown.

CONCLUSION

In summary, we have developed a targeted NP platform for cancer therapy by incorporating Apts isolated from a novel cell-uptake selection process. The selection was uniquely designed to enrich cancer

cell-specific internalizing Apts rather than highest affinity Apts as reported in previous selection processes. After modifying NPs with these selected Apts, the NP−Apt conjugates demonstrated enhanced therapeutic efficacy in target cancer cells. Further engineering of NPs with a diverse pool of Apts would facilitate the development of multi-ligand-targeted NP platforms. In this platform, detailed knowledge of the target antigens on the cell surface is not needed, simplifying the process of targeted NP development. Further characterization of the target antigens may lead to the discovery of important PCa biomarkers. This internalizing NP−Apt platform can be similarly applied in a wide variety of other oncologic diseases and can potentially facilitate the delivery of various molecules, including drugs and siRNAs, into target cells.

METHODS

Cell Lines. LNCaP, PC3, SKBR3, HeLa, RWPE-1, A375, U373MG, T98G, U-87MG, A549, and SKOV-3 were from ATCC (Manassas). BPH-1 was from Vanderbilt University Medical Center (Nashville). PrEC was from Cambrex (Hopkinton). Cells were grown according to the manufacturer's specifications. All cell lines were used within three to ten passages from their acquisition. The internal authentication has been performed by monitoring growth rate and tracking the changes in morphology.

RNA Library and Primers. The DNA library ($\sim 9 \times 10^{14}$) 5′-CATCGATGCTAGTCGTAACGATCC-30N-CGAGAACGTTTCTCTCC-TCTCCCTATAGTGAGTCGTATTA-3′ (Operon) was amplified by PCR (5 min at 95 °C, followed by cycles of 0.5 min at 95 °C, 0.5 min at 65 °C, and 1 min at 72 °C, followed by 2 min at 72 °C), with reverse primer 5′-CATCGATGCTAGTCGTAACGATCC-3′ and forward primer 5′-TAATACGACTCACTATAGGGAGAGGAGAGAAA-CGTTCTCG-3′. The resultant dsDNAs were precipitated and separated by gel filtration. Partly 2′-OMe-modified RNAs were obtained by overnight incubation at 37 °C of the reaction mixture: 200 nM template, 200 mM HEPES, 40 mM DTT, 10% PEG_{8000}, 0.01% Triton X-100, 2 mM spermidine, 1.0 mM each of GTP, 2′-OMe-ATP, 2′-OMe-CTP, and 2′-OMe-UTP (Trilink), 5.5 mM $MgCl_2$, 1.5 mM $MnCl_2$, 10 U/mL inorganic pyrophosphatase (Sigma-Aldrich), and 200 nM T7 RNA polymerase.[24] The resultant transcripts were precipitated in 3 M LiCl at −80 °C, followed by ethanol precipitation.

Cell-Uptake Selection. The RNA library (1.5 nmol) was briefly denatured at 90 °C in 20 mL of selection buffer (EBSS with 1 mM $MgCl_2$), cooled slowly, and then warmed up to 37 °C before consecutive incubations with three counter-selection cell lines (RWPE-1, BPH-1, and PrEC). After each incubation (60 min for the first 5 rounds, 45 min afterward), the unbound RNAs were collected for the next incubation. After consecutive incubations with these three counter-selection cells, the pool was exposed to the positive-selection cells, LNCaP or PC3, with varied incubation time: 60 min for rounds 1−2, 45 min for rounds 3−5, and 30 min for rounds 6−12. The cells were then extensively washed (rounds 1−12) and either lysed to collect the internalized RNAs (rounds 1−6) or treated with trypsin to remove the membrane-bound RNAs prior to cell lysis for the collection of internalized RNAs (rounds 7−12). The internalized RNAs were then extracted using Trizol reagent (Invitrogen). Selected RNAs were treated with RQ1 DNase (Promega), before reverse transcription and PCR amplification. To monitor the enrichment of internalizing Apt candidates, a semiquantitiative PCR method was used to quantify the numbers of PCR cycles carried out to obtain the same amount of PCR products. Briefly, the collected reverse-transcribed DNAs of each round were equivalently separated into several reaction tubes and simultaneously run through different numbers of PCR cycles. The products were loaded in parallel on the agarose gel and quantified by the intensity of specific bands. The experiments were repeated three times to determine the number of cycles necessary to achieve a given amount. The PCR reaction was then repeated by running the desired number of PCR cycles. Subsequently, the PCR products were purified, transcribed into modified RNA, treated with DNase and precipitated with LiCl, followed by ethanol precipitation before starting the next cycle. During the selection, the number of PC3 and LNCaP cells exposed to the RNA library progressively decreased, starting with 1×10^7 and diminishing by $1-2 \times 10^6$ cells every other round until reaching 1×10^6 for round 12. After 7 rounds of selection, the material was amplified with 14 cycles of mutagenic PCR (template DNA = 25 μg/μL; $MgCl_2$ = 7 mM; Tris = 10 mM; KCl = 50 mM; primers = 2 M; dCTP and dTTP = 1 mM; dGTP and dATP = 0.2 mM; enzyme = 0.05 U/L; and $MnCl_2$ = 0.5 mM; annealing 3 min) to introduce occasional mutations (roughly 0.79% mutations per position; 0.24% mutations per sequence). After 12 rounds of selection, sequences were cloned into the pCR-4 TOPO plasmid, using the TOPO-TA cloning kit (Invitrogen).

Identification of Selected Pools. To identify the internalization of selected RNA pools, NBD-encapsulated NPs with maleimide groups were prepared using the combination of self-assembly and nanoprecipitation method as previously described.[26] The RNA pool was then oxidized to form aldehyde derivatives, and cystamine was incubated with RNA for 2 h to functionalize the RNA with a free thiol reacting group. Subsequently, sodium sulfite (2×) was added to remove the excess oxidant and cystamine. NPs were further incubated with RNAs for 12 h at room temperature with gentle stirring to form NP−RNA conjugates. For confocal imaging, cells were incubated with NP-(NBD)−RNA conjugates in selection buffer for 1 h, washed, fixed with 4% formaldehyde, followed by 0.1% Triton-X100, stained with rhodamine-phalloidin, and mounted with DAPI. Cells were visualized with 1.4 NA oil immersion 25× or 60× objectives, and individual images were taken along their *z*-axis at 0.1 μm intervals with a confocal microscope (Carl Zeiss).

Measurement of Apt Binding Affinity. The binding affinity of XEO2 Apt was determined by incubating PC3 cells (5×10^5) at 37 °C for 30 min in the dark with varying concentrations of Cy3-labeled Apts in a 500 μL volume of binding buffer. Cells were then washed twice with 700 μL of the binding buffer with 0.1% sodium azide, suspended in 400 μL of binding buffer with 0.1% sodium azide, and subjected to flow cytometric analysis within 30 min. The Cy3-labeled unselected RNA library was used as a negative control to determine nonspecific binding. All of the experiments for the binding assay were repeated two times. The mean fluorescence intensity of target cells labeled by Apts was used to calculate specific binding by subtracting the mean fluorescence intensity of nonspecific binding from unselected library RNAs. The equilibrium dissociation constants (K_d) of the Apt−cell interaction were obtained by fitting the dependence of fluorescence intensity of specific binding on the concentration of the Apts to the equation $Y = B_{max}X/(K_d + X)$, using SigmaPlot (Jandel, San Rafael, CA).

Internalization Characterization of Selected Apts. All of the specific sequence candidates and initial libraries were synthesized by a solid-phase process and were directly conjugated with Cy3 at the 5′-end (Thermo Sci.), followed by purification using reverse-phase RNA enzyme-free HPLC. For flow cytometry analysis, Cy3-labeled Apts were heated at 95 °C for 5 min, then slowly cooled to room temperature for 2 h. Cells (10^5) were then incubated with a serial concentration of Cy3-labeled Apts (125 nM to 4 μM for upake efficacy analysis, and 3 μM for cell-specific analysis) in 500 μL of binding buffer [4.5 g/L glucose, 1 mM $MgCl_2$, 0.1 mg/mL yeast tRNA, and 1 mg/mL BSA in EBSS] at 37 °C for 2 h. After washing with 700 μL of binding buffer (with 0.1% NaN_3), cells were incubated with prewarmed trypsin (500 μL, 0.25%)/EDTA (0.53 mM) at 37 °C for 10 min. Subsequently, FBS (50 μL) was added, and cells were centrifuged. The cell pellets were washed

with binding buffer (700 μL, with 0.1% NaN_3) once again and suspended in 300 μL of binding buffer (with 0.1% NaN_3). The fluorescence was determined with a FACScan cytometer (Accuri C6 cytometers) by counting 20 000 events (note: only living cells were counted). For confocal imaging, cells (10^4) were washed and incubated with Cy3-labeled Apts (200 nM) in binding buffer at 37 °C for 2 h. After extensive washing with cold binding buffer three times, the cells were fixed and kept in dark before imaging.

Proteinase Treatment for Cells. Cell monolayers were detached by non-enzymatic cell dissociation solution (Invitrogen Corporation, Carlsbad, CA), filtered with a 40 μm cell strainer (Becton, Dickinson and Company, Franklin Lakes, NJ). PC3 or LNCaP cells (2×10^5) were incubated with 500 μL of 0.25% trypsin/0.53 mM EDTA in HBSS or 0.1 mg/mL proteinase K in PBS at 37 °C for 2 and 10 min. FBS was then immediately added to quench the proteinase digestion. After washing with 700 μL of binding buffer, the treated cells were incubated with Cy3-labeled Apt (1 μM) in a 500 μL volume of binding buffer at 37 °C for 30 min. Cells were then washed twice with 700 μL of prewarmed binding buffer (with 0.1% NaN_3) and suspended in 300 μL of binding buffer. The cell suspension was transferred into FACS tube with 40 μm cell strainer cap (Becton, Dickinson and Company, Franklin Lakes, NJ) and subjected to flow cytometric analysis within 30 min. The Cy3-labeled Apt under the same condition, but without proteinase treatment, was applied in showing cell-specific binding profile.

Cellular Uptake and Cytotoxicity Study of NP–Apt Conjugates. NPs were first prepared *via* nanoprecipitation and self-assembly.[26] To form NP–Apt conjugates the disulfide-terminated Apt XEO2 mini was synthesized by Integrated DNA Technology (IDT), followed by reduction with 5 mM of TCEP (neutral pH, Thermo Scientific) in PBS (pH 7.4) for 30 min at room temperature. Free TCEP was removed by a G-25 Sephadex column (Roche Diagnostics). Apt was added into the prepared NPs and incubated for 2 h with gentle stirring, followed by washing with Amicon tubes. To identify the specific cellular uptake of NP–Apt conjugates, PC3 or HeLa cells (10^5) were incubated with prewarmed binding buffer for 30 min and then further incubated with 0.5 mg/mL NP–Apt (NBD) or NP (NBD) at 37 °C for 30 min. For cytotoxicity studies, the PC3 and HeLa cells (8×10^3) were seeded in 96-well plates to allow growth for 24 h. On the day of the experiment, the cells were washed once and incubated with prewarmed binding buffer for 30 min. With the addition of Dtxl–NP–Apt, Dtxl–NP (100 μg/mL, Dtxl with 5% weight ratio of PLGA), and Apt XEO2 mini (2.5 μM), the cells were further incubated in binding buffer for 30 min. The cells were then washed twice, and fresh media were added for further growth for 48 h. Cell viability was measured by MTT cell proliferation assay kits (Invitrogen).

Acknowledgment. E.L.-N. dedicates this work in memory of Emilia Levy. We thank Jack W. Szostak, Brian Haines, and Noam Shomron for helpful discussions and suggestions. We thank Rosa Larralde-Ridaura for helping with the sequence identification. This research was supported by National Institutes of Health Grants CA151884 and EB003647, the David Koch—Prostate Cancer Foundation Award in Nanotherapeutics, and the USA Department of Defence Prostate Cancer Research Program PC 051156. R.L. and O.C.F. disclose their financial interest in BIND Biosciences and Selecta Biosciences, two biotechnology companies developing nanoparticle technologies for medical applications.

Supporting Information Available: Figures for selection progress identified by the number of PCR cycles, predicted secondary structures of Apts XEO2 and XEO6, XEO2 mini internalization by flow cytometry and confocal analysis, binding curve of Apt XEO2; internalization profiles of XEO2 and A10 in LNCaP cells, effects of proteinase K or trypsin treatment on XEO9 and XEO2 mini binding profile, targeted delivery of NP-XEO2 mini (NBD) by flow cytometry analysis, and cytotoxicity study of Apt XEO2 mini in PC3 cells and HeLa cells. This material is available free of charge *via* the Internet at http://pubs.acs.org.

REFERENCES AND NOTES

1. Davis, M. E.; Chen, Z. G.; Shin, D. M. Nanoparticle Therapeutics: An Emerging Treatment Modality for Cancer. *Nat. Rev. Drug Discovery* **2008**, *7*, 771–782.
2. Langer, R. Drug Delivery and Targeting: Review. *Nature* **1998**, *392*, 5–10.
3. Farokhzad, O. C.; Cheng, J.; Teply, B. A.; Sherifi, I.; Jon, S.; Kantoff, P. W.; Richie, J. P.; Langer, R. Targeted Nanoparticle-Aptamer Bioconjugates for Cancer Chemotherapy *in Vivo*. *Proc. Natl. Acad. Sci. U.S.A.* **2006**, *103*, 6315–6320.
4. Sugano, M.; Egilmez, N. K.; Yokota, S. J.; Chen, F. A.; Harding, J.; Huang, S. K.; Bankert, R. B. Antibody Targeting of Doxorubicin-Loaded Liposomes Suppresses the Growth and Metastatic Spread of Established Human Lung Tumor Xenografts in Severe Combined Immunodeficient Mice. *Cancer Res.* **2000**, *60*, 6942–6949.
5. Sapra, P.; Allen, T. M. Internalizing Antibodies Are Necessary for Improved Therapeutic Efficacy of Antibody-Targeted Liposomal Drugs. *Cancer Res.* **2002**, *62*, 7190–7194.
6. Park, J. W.; Hong, K.; Kirpotin, D. B.; Colbern, G.; Shalaby, R.; Baselga, J.; Shao, Y.; Nielsen, U. B.; Marks, J. D.; Moore, D. Anti-Her2 Immunoliposomes: Enhanced Efficacy Attributable to Targeted Delivery. *Clin. Cancer Res.* **2002**, *8*, 1172–1181.
7. Whitehead, K. A.; Langer, R.; Anderson, D. G. Knocking down Barriers: Advances in SiRNA Delivery. *Nat. Rev. Drug Discovery* **2009**, *8*, 129–138.
8. Petros, R. A.; DeSimone, J. M. Strategies in the Design of Nanoparticles for Therapeutic Applications. *Nat. Rev. Drug Discovery* **2010**, *9*, 615–627.
9. Sawyers, C. L. The Cancer Biomarker Problem. *Nature* **2008**, *452*, 548–552.
10. Cao, Z.; Tong, R.; Mishra, A.; Xu, W.; Wong, G. C.; Cheng, J.; Lu, Y. Reversible Cell-Specific Drug Delivery with Aptamer-Functionalized Liposomes. *Angew. Chem., Int. Ed.* **2009**, *48*, 6494–6498.
11. Farokhzad, O. C.; Jon, S.; Khademhosseini, A.; Tran, T. N.; Lavan, D. A.; Langer, R. Nanoparticle–Aptamer Bioconjugates: A New Approach for Targeting Prostate Cancer Cells. *Cancer Res.* **2004**, *64*, 7668–7672.
12. Bouchard, P. R.; Hutabarat, R. M.; Thompson, K. M. Discovery and Development of Therapeutic Aptamers. *Annu. Rev. Pharmacol. Toxicol.* **2010**, *50*, 237–257.
13. Keefe, A. D.; Pai, S.; Ellington, A. Aptamers as Therapeutics. *Nat. Rev. Drug Discovery* **2010**, *9*, 537–550.
14. Ellington, A. D.; Szostak, J. W. *In Vitro* Selection of RNA Molecules That Bind Specific Ligands. *Nature* **1990**, *346*, 818–822.
15. Tuerk, C.; Gold, L. Systematic Evolution of Ligands by Exponential Enrichment: RNA Ligands to Bacteriophage T4 DNA Polymerase. *Science* **1990**, *249*, 505–510.
16. Daniels, D. A.; Chen, H.; Hicke, B. J.; Swiderek, K. M.; Gold, L. A Tenascin-C Aptamer Identified by Tumor Cell Selex: Systematic Evolution of Ligands by Exponential Enrichment. *Proc. Natl. Acad. Sci. U.S.A.* **2003**, *100*, 15416–15421.
17. Shangguan, D.; Li, Y.; Tang, Z.; Cao, Z. C.; Chen, H. W.; Mallikaratchy, P.; Sefah, K.; Yang, C. J.; Tan, W. Aptamers Evolved from Live Cells as Effective Molecular Probes for Cancer Study. *Proc. Natl. Acad. Sci. U.S.A.* **2006**, *103*, 11838–11843.
18. Raddatz, M. S.; Dolf, A.; Endl, E.; Knolle, P.; Famulok, M.; Mayer, G. Enrichment of Cell-Targeting and Population-Specific Aptamers by Fluorescence-Activated Cell Sorting. *Angew. Chem., Int. Ed.* **2008**, *47*, 5190–5193.
19. Sefah, K.; Shangguan, D.; Xiong, X.; O'Donoghue, M. B.; Tan, W. Development of DNA Aptamers Using Cell-Selex. *Nat. Protoc.* **2010**, *5*, 1169–1185.
20. Xiao, Z.; Shangguan, D.; Cao, Z.; Fang, X.; Tan, W. Cell-Specific Internalization Study of an Aptamer from Whole Cell Selection. *Chemistry* **2008**, *14*, 1769–1775.
21. Wu, Y.; Sefah, K.; Liu, H.; Wang, R.; Tan, W. DNA Aptamer-Micelle as an Efficient Detection/Delivery Vehicle toward Cancer Cells. *Proc. Natl. Acad. Sci. U.S.A.* **2010**, *107*, 5–10.
22. Pieken, W. A.; Olsen, D. B.; Benseler, F.; Aurup, H.; Eckstein, F. Kinetic Characterization of Ribonuclease-Resistant 2′-Modified Hammerhead Ribozymes. *Science* **1991**, *253*, 314–317.
23. Liu, B.; Conrad, F.; Cooperberg, M. R.; Kirpotin, D. B.; Marks, J. D. Mapping Tumor Epitope Space by Direct Selection of Single-Chain Fv Antibody Libraries on Prostate Cancer Cells. *Cancer Res.* **2004**, *64*, 704–710.

24. Burmeister, P. E.; Lewis, S. D.; Silva, R. F.; Preiss, J. R.; Horwitz, L. R.; Pendergrast, P. S.; McCauley, T. G.; Kurz, J. C.; Epstein, D. M.; Wilson, C. Direct *In Vitro* Selection of a 2-O-Methyl Aptamer to Vegf. *Chem. Biol.* **2005**, *12*, 25–33.
25. Cadwell, R. C.; Joyce, G. F. Randomization of Genes by PCR Mutagenesis. *PCR Methods Appl.* **1992**, *2*, 28–33.
26. Zhang, L.; Chan, J. M.; Gu, F. X.; Rhee, J. W.; Wang, A. Z.; Radovic-Moreno, A. F.; Alexis, F.; Langer, R.; Farokhzad, O. C. Self-Assembled Lipid−Polymer Hybrid Nanoparticles: A Robust Drug Delivery Platform. *ACS Nano* **2008**, *2*, 1696–1702.
27. Chan, J. M.; Zhang, L.; Yuet, K. P.; Liao, G.; Rhee, J. W.; Langer, R.; Farokhzad, O. C. PLGA-Lecithin-PEG Core−Shell Nanoparticles for Controlled Drug Delivery. *Biomaterials* **2009**, *30*, 1627–1634.
28. Chan, J. M.; Zhang, L.; Tong, R.; Ghosh, D.; Gao, W.; Liao, G.; Yuet, K. P.; Gray, D.; Rhee, J. W.; Cheng, J.; *et al.* Spatiotemporal Controlled Delivery of Nanoparticles to Injured Vasculature. *Proc. Natl. Acad. Sci. U.S.A.* **2010**, *107*, 2213–2218.
29. Wu, C. C. N.; Castro, J. E.; Motta, M.; Cottam, H. B.; Kyburz, D.; Kipps, T. J.; Corr, M.; Carson, D. A. Selection of Oligonucleotide Aptamers with Enhanced Uptake and Activation of Human Leukemia B Cells. *Hum. Gene Ther.* **2003**, *14*, 849–860.
30. Perera, R. M.; Zoncu, R.; Johns, T. G.; Pypaert, M.; Lee, F. T.; Mellman, I.; Old, L. J.; Toomre, D. K.; Scott, A. M. Internalization, Intracellular Trafficking, and Biodistribution of Monoclonal Antibody 806: A Novel Anti-Epidermal Growth Factor Receptor Antibody. *Neoplasia* **2007**, *9*, 1099–1110.
31. Nguyen, H. M.; Cahill, C. M.; McPherson, P. S.; Beaudet, A. Receptor-Mediated Internalization of [3h]-Neurotensin in Synaptosomal Preparations from Rat Neostriatum. *Neuropharmacology* **2002**, *42*, 1089–1098.
32. Larkin, S. E.; Zeidan, B.; Taylor, M. G.; Bickers, B.; Al-Ruwaili, J.; Aukim-Hastie, C.; Townsend, P. A. Proteomics in Prostate Cancer Biomarker Discovery. *Expert Rev. Proteomics* **2010**, *7*, 93–102.
33. Heppner, G. H. Tumor Heterogeneity. *Cancer Res.* **1984**, *44*, 2259–2265.
34. Rajan, P.; Elliott, D. J.; Robson, C. N.; Leung, H. Y. Alternative Splicing and Biological Heterogeneity in Prostate Cancer. *Nat. Rev. Urol.* **2009**, *6*, 454–460.
35. O'Keefe, D. S.; Bacich, D. J.; Heston, W. D. Comparative Analysis of Prostate-Specific Membrane Antigen (PSMA) *versus* a Prostate-Specific Membrane Antigen-like Gene. *Prostate* **2004**, *58*, 200–210.
36. Liu, H.; Moy, P.; Kim, S.; Xia, Y.; Rajasekaran, A.; Navarro, V.; Knudsen, B.; Bander, N. H. Monoclonal Antibodies to the Extracellular Domain of Prostate-Specific Membrane Antigen Also React with Tumor Vascular Endothelium. *Cancer Res.* **1997**, *57*, 3629–3634.
37. Chang, S. S.; Reuter, V. E.; Heston, W. D. W.; Bander, N. H.; Grauer, L. S.; Gaudin, P. B. Five Different Anti-Prostate-Specific Membrane Antigen (PSMA) Antibodies Confirm PSMA Expression in Tumor-Associated Neovasculature. *Cancer Res.* **1999**, *59*, 3192–3198.
38. Gu, F.; Zhang, L.; Teply, B. A.; Mann, N.; Wang, A.; Radovic-Moreno, A. F.; Langer, R.; Farokhzad, O. C. Precise Engineering of Targeted Nanoparticles by Using Self-Assembled Biointegrated Block Copolymers. *Proc. Natl. Acad. Sci. U.S.A.* **2008**, *105*, 2586–2591.
39. Istomin, Y. P.; Zhavrid, E. A.; Alexandrova, E. N.; Sergeyeva, O. P.; Petrovich, S. V. Dose Enhancement Effect of Anticaner Drugs Associated with Increased Temperature *in Vitro*. *Exp. Oncol.* **2008**, *30*, 56–59.
40. Fizazi, K.; Sikes, C. R.; Kim, J.; Yang, J.; Martinez, L. A.; Olive, M. C.; Logothetis, C. J.; Navone, N. M. High Efficacy of Docetaxel with and without Androgen Deprivation and Estramustine in Preclinical Models of Advanced Prostate Cancer. *Anticancer Res.* **2004**, *24*, 2897–2903.
41. Takara, K.; Sakaeda, T.; Yagami, T.; Kobayashi, H.; Ohmoto, N.; Horinouchi, M.; Nishiguchi, K.; Okumura, K. Cytotoxic Effects of 27 Anticancer Drugs in HeLa and Mdr1-Overexpressing Derivative Cell Lines. *Biol. Pharm. Bull.* **2002**, *25*, 771–778.